# Snatch loading of a single taut moored floating wave energy converter due to focussed wave groups

Hann, Martyn; Greaves, Deborah; Raby, Alison

**Published in:**
Ocean Engineering

**DOI:**
10.1016/j.oceaneng.2014.11.011

**Publication date:**
2015

**Document version:**
Publisher's PDF, also known as Version of record

Ocean Engineering 96 (2015) 258–271

Contents lists available at ScienceDirect

Ocean Engineering

journal homepage: www.elsevier.com/locate/oceaneng

# Snatch loading of a single taut moored floating wave energy converter due to focussed wave groups

Martyn Hann*, Deborah Greaves, Alison Raby

*School of Marine Science and Engineering, Plymouth University, UK*

ARTICLE INFO

*Article history:*
Received 21 September 2013
Accepted 30 November 2014

*Keywords:*
NewWave
Wave impact
Moorings
Snatch loading
Wave energy converter
Survivability

ABSTRACT

This paper concerns experimental measurements of the interaction of a taut moored floating body, representing a wave energy converter in survivability mode, with extreme waves. Focussed wave groups, based initially on NewWave theory, are used to generate the extreme waves, with crest amplitude exceeding the mooring's design capacity. Two data sets are presented and discussed. In the first the influence of wave steepness on model response and mooring load is investigated using non-breaking focussed wave groups. In the second the influence of wave breaking location is investigated using a plunging breaking wave. Both data sets exhibit snatch loading as the extension of the mooring is exceeded. The magnitude of this loading is not found to be strongly dependent on wave steepness, while the following motion response of the body is. Breaking location has a much greater effect than wave steepness on the magnitude of the mooring load, while significant influence of the body motion and displacement on the mooring load is demonstrated. Evidence is provided that the use of individual focussed wave groups is inadequate to assess fully the extreme loads experienced by a taut moored WEC due to the demonstrated dependence of mooring load on the body's motion and displacement.



## 1. Introduction

Regardless of their location in the ocean, wave energy converters (WECs) have two primary requirements: to provide efficient conversion in small to moderate seas and to survive storm conditions (Barstow et al., 2008, p. 52). An important factor to consider when assessing the ability of a device to survive storms is its response when hit by an extreme wave. The accurate prediction of extreme loading due to waves is therefore important in the design process of a WEC.

One approach that can be used to estimate the response is by conducting scaled experiments of the WEC in storm sea conditions. This requires long duration runs before a statistically reliable assessment of the extreme loading can be made. Such approaches are expensive, both in terms of time and facility use, and can be difficult to implement accurately due to the increasing influence of wave reflections.

An alternative approach for measuring extreme responses at scale is the use of focussed wave groups. These are generated by adjusting the phase relationship between wave components of different frequencies so that a concentration of energy is achieved at a specified time and location in the tank. Zhao and Hu (2012) use this technique to measure the interactions of an extreme wave with a floating body constrained to move in heave and pitch only.

A specific type of focussed wave group was introduced by Tromans et al. (1991) and is called NewWave. NewWave theory produces, for a given sea state, the average shape of the highest wave with a specified exceedance probability (Xu et al., 2008). This design wave has been used experimentally and numerically in various applications. Rozario et al. (1993) successfully compared the loads predicted by NewWave on a North Sea oil platform with simulations of random seas. Borthwick et al. (2006) measured wave kinematics of NewWaves impacting on a 1:20 beach plane, while Hunt-Raby et al. (2011) measured wave overtopping of embankments. The interaction of fixed cylinders with NewWaves has been studied to assess extreme wave impacts, relevant for a wide range of offshore structures (Walker and Eatock Taylor, 2005; Stallard et al. 2009a; Ransley et al., 2013; Zang et al., 2010).

NewWave groups have also been used previously to study extreme loading on floating devices. Stallard et al. (2009b) used this form of focussed wave to measure the response of a float suitable for a wave energy converter in extreme waves. In this study the float was not moored, but instead a fixed force was applied to the float, initially vertically, using a mass attached via a pulley above the float. Xu et al. (2008) studied extreme loading on

* Correspondence to: Marine Building 2nd floor, Plymouth University, Drake Circus, Plymouth, Devon, PL4 8AA, UK.
*E-mail address:* mr.hann@ntlworld.com (M. Hann).

http://dx.doi.org/10.1016/j.oceaneng.2014.11.011

the bow of an FPSO (Floating Production Storage and Offloading vessel) using NewWave theory, extending the theory to generate steep waves. Taylor et al. (1997) conducted simulations using a NewWave embedded into a random wave sequence to estimate the extreme response of a Jack-up. This simulated the effect of load history and structural dynamics which are not present when using an individual focussed wave group. Taylor et al. (1997) predict that for a dynamically-responding structure the extreme response does not necessarily correspond to the extreme surface elevation. This study has shown this to be the case.

In the experiments reported here focussed wave groups, based initially on NewWave theory, have been applied to measure the response of a generic wave energy converter to extreme waves. A single taut moored floating point absorber, representing devices such as the CETO, AWS (Stallard et al., 2009b), SeaBeav1 (Elwood et al., 2011) and the Uppsala University WEC (Waters et al., 2007), has been tested. The mooring was designed so that its extension was insufficient to fully accommodate the waves tested and extreme loads were hence generated in the mooring line and anchor. Full scale moorings are designed to try and avoid this form of loading due to the potential damage it can cause. These extreme loads reflect a worst-case scenario which these experiments aimed to investigate.

Two series of tests have been conducted. In the first a NewWave wave group was focussed at the front face of the device at its initial position. The steepness of this wave group was then increased, up to just before the wave breaks, while maintaining the physical location at which the group was focussed. This allowed the effect of wave steepness on the model's response to be assessed. The second series of tests investigated the response of the model to a plunging breaking wave. These were generated by increasing the steepness of the wave group further. A series of tests were conducted varying the theoretical focus location of the wave group so that the plunging breaker formed at different locations relative to the device. Repeat experiments were conducted to ascertain variability of the measurements.

In both test series the motion of the model and the mooring loads were recorded. By measuring the dependence of motion and loads on both wave steepness and breaking point an assessment could be made of the validity of using single focussed wave groups to measure extreme wave impacts on a single taut moored floating body. The data is also being used to validate a CFD numerical model of a floating WEC.

These measurements were conducted as part of the EPRSC X-MED project (Extreme loading of marine energy devices due to waves, current, flotsam and mammal impacts). They were also the first measurements to be conducted at Plymouth University's ocean basin (COAST Lab, 2013).

## 2. Experimental methodology

### 2.1. Model wave energy converter

There is a wide range of variability in the design of wave energy converters. Clément et al. (2002) stated that over 1000 wave energy conversion techniques were patented in Japan, North America and Europe by 2002, while over the last decade the development of device concepts has continued. These devices can be classified according to where they operate (Polinder and Scuotto, 2005; Barstow el al., 2008, p. 46). Shoreline devices include devices mounted on shore or on the seabed in shallow water and near-shore devices operate in 10–20 m water depths and up to a kilometre from the shore. This research is primarily concerned with the third category of devices, those in the offshore environment, which contains the most energetic wave climate. Offshore devices therefore have the potential to extract most energy, but are also exposed to the most extreme conditions during storms.

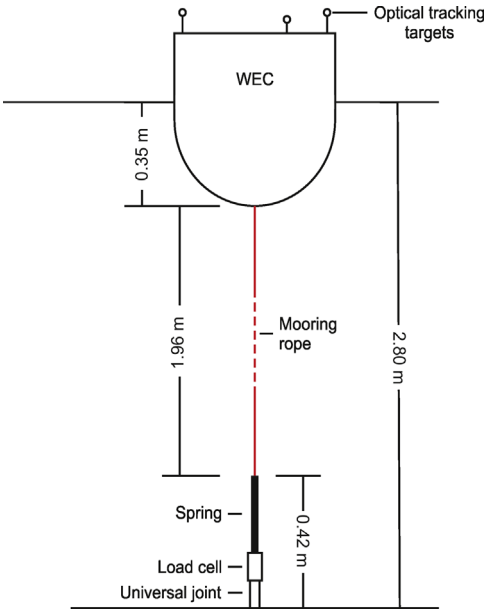


**Fig. 1.** Model set-up and instrumentation.

Devices can also be classified according to working principle. Falcão (2010) identifies 3 categories of devices: oscillating water columns, oscillating bodies and overtopping devices, each with a number of sub-categories. This study has been conducted on a floating body designed to represent a floating oscillating water column or floating oscillating body. Even within these subcategories there is a wide variability in both design and mooring arrangement, and in order to ensure that results are generally applicable, a simple buoy representing a generic WEC has been selected for investigation.

The design of the model is shown in Fig. 1. It is a 0.5 m diameter hemispherical floating body with a single taut mooring and a dry mass of 43.2 kg. The mooring consists of 1.96 m of Dyneema® rope (spring constant, $k \approx 35$ N/mm) in series with a linear spring ($k = 0.064$ N/mm), which provides the mooring's extension. Four lengths of the same rope act as end-stops for the spring, preventing it from being overextended (Fig. 2). The initial and maximum lengths of the spring are 152 mm and 406 mm respectively. In still water the spring was extended to 257 mm, giving a further possible extension of 149 mm, 56% of the theoretical main wave crest of the initial NewWave (Fig. 3). This mooring arrangement is similar to that used by Eriksson et al. (2006) during full scale tests on a cylindrical buoy designed for use as a wave energy converter.

A model power take-off (PTO) has not been incorporated into the experimental set-up for a number of reasons. Firstly the wide range in design and properties of PTOs used by different devices would make modelling a meaningful 'generic' PTO difficult. Secondly some devices lock the PTO or disconnect from it during storms to avoid damage. Finally, this research is concerned with assessing the most extreme device reactions. Including a model PTO would extract energy and potentially damp the response of the device (Stallard et al., 2009b), which would therefore not represent the extreme.

A series of decay tests were conducted on the model and mooring system to measure its resonance frequencies. These were found to be 0.93 Hz for heave, 0.68 Hz for pitch and 0.04 Hz for surge.

### 2.2. Experimental layout and instrumentation

Measurements were conducted in a 35 m × 15.5 m ocean basin at Plymouth University's COAST laboratory. The variable floor depth

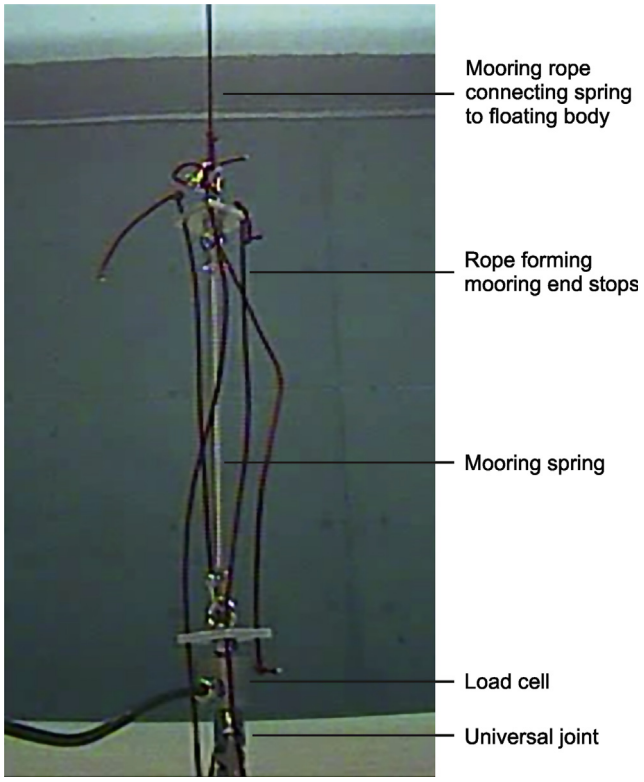


**Fig. 2.** Mooring spring arrangement.

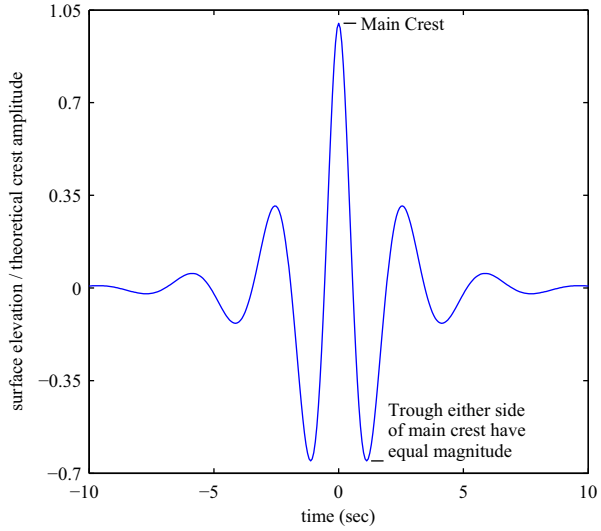


**Fig. 3.** Theoretical NewWave generated by a Pierson–Moskowitz (PM) spectrum, demonstrating the symmetry of the group around the main crest.

was set at 2.8 m. The facility has 24 2.0 m deep hinged wave paddles across one side of the tank. Wave reflections are reduced using a parabolic beach and the wave paddles active absorption.

The model was moored, in its resting position, along the centre line of the basin, 18.8 m from the front of the wave paddles. A series of 16 resistance type wave gauges were positioned along the same central line for tests prior to the model being installed (the locations of which are given in Table 1). These were used to measure the propagation of the focussed wave group and, for the breaking waves, to identify the breaking point of the wave relative

**Table 1**
Location of wave gauges (WG) relative to wave paddles ($x_{paddles}$) and the centre of the model's resting position ($x_{model}$).

| WG# | 1 | 2 | 3 | 4 | 5 | 6 |
|---|---|---|---|---|---|---|
| $x_{paddles}$ (m) | 13.18 | 13.93 | 14.39 | 14.86 | 15.31 | 15.66 |
| $x_{model}$ (m) | −5.58 | −4.83 | −4.37 | −3.90 | −3.45 | −3.10 |
| WG# | 7 | 8 | 9 | 10 | 11 | 12 |
| $x_{paddles}$ (m) | 15.97 | 16.32 | 16.76 | 17.11 | 17.46 | 17.81 |
| $x_{model}$ (m) | −2.80 | −2.45 | −2.00 | −1.65 | −1.30 | −0.95 |
| WG# | 13 | 14 | 15 | 16 | | |
| $x_{paddles}$ (m) | 18.17 | 18.51 | 18.86 | 19.21 | | |
| $x_{model}$ (m) | −0.59 | −0.25 | 0.10 | 0.45 | | |

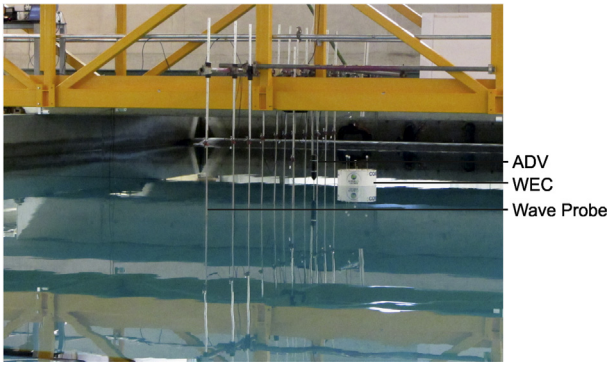


**Fig. 4.** Experimental layout with model WEC installed.

to the initial position of the moored device. Wave gauges 12–16 were then removed to make way for the model to be installed (Fig. 4).

Acoustic Doppler velocimeter (ADV) measurements were conducted alongside the 11th wave gauge. These measurements of fluid velocity were taken for comparison with CFD modelling and are not presented here.

The motion of the device in response to wave interactions was measured using a Qualisys optical tracking system with 4 Qualisys Oqus 300+ cameras. This provides a record of the six degrees of freedom response, which, unless otherwise stated, was translated to a point at the centre of the device on the initial water-line. The waves measured are all long crested and normally-incident and hence roll, yaw and sway response of the device are minimal and are not presented here. The maximum measured residual in the optical tracking was ±0.5 mm. Mooring loads were measured with a 5 kN in-line tension and compression load cell (Applied measurements Ltd. DDENA1S – 5000N – C15) attached between a universal joint, used to anchor the mooring to the basin floor, and the spring (Fig. 2).

### 2.3. Focussed wave group generation

The Pierson–Moskowitz (PM) spectrum was used as the underlying spectrum of the initial NewWave. The input to the spectrum was based on hindcast data for a 100-year storm at Wave Hub, a wave energy test facility off the north Cornwall coast in the south west of the UK ($T_z$=14.1 s, $H_s$=14.4 m, Halcrow, 2006). The wave was generated at 50th scale. From NewWave theory the amplitude ($A$) of the largest in $N$ waves is given by

$$A = \sqrt{2m_0 \ln(N)}, \quad (1)$$

**Table 2**
Properties of the non-breaking wave groups tested.

| *Case* | *Theoretical kA* | Peak frequency multi-factor | Theoretical focus (m) ($x_{focus\_th}$) |
|---|---|---|---|
| ST1 | 0.15 | 1.00 | 18.3 |
| ST2 | 0.175 | 1.09 | 17.7 |
| ST3 | 0.20 | 1.18 | 17.2 |
| ST4 | 0.225 | 1.26 | 16.8 |

where $m_0$ is the zeroth moment of the spectrum. In a 3 h sea state there are approximately 1000 waves (Hunt-Raby et al., 2011). Taking this for the value of $N$ gives crest amplitude, $A=0.267$ m.

A series of waves with frequencies between 0.10 and 2.0 Hz (the generation capacity of the COAST laboratory's ocean basin) were used to generate the initial NewWave. Wave amplitudes of the individual frequency components were determined using NewWave theory. In order to assess the effect of wave steepness on the WEC response, the steepness of the wave group was increased by multiplying the original peak frequency ($f_p$) used to generate the NewWave (0.356 Hz) by a particular factor. Note that these steeper wave groups can no longer be considered as NewWave groups as the relationship between the input spectrum and amplitude is no longer given by Eq. (1). Four different wave groups of increasing steepness were identified, before the occurrence of breaking. The theoretical steepness of these wave groups, and the factors by which the peak frequency was multiplied by to achieve these steepnesses, are given in Table 2. Wave steepness ($kA$) was calculated using the wave number ($k$) corresponding to the peak frequency of the resulting wave groups spectrum (assuming linear wave theory). The initial NewWave is the wave group with a steepness of $kA=0.15$.

This approach to increasing the steepness of the wave group has the disadvantage of modifying wave excitation frequency relative to the resonance frequencies of the model. The effect of this is discussed in greater detail below. An alternative approach to increase wave steepness would have been to fix the spectrums peak frequency and increase the crest amplitude ($A$). This approach would have increased mooring load due to the extra heave a greater wave amplitude would produce, therefore limiting any conclusions that could be made regarding the effect of wave steepness.

All four non-breaking wave groups were focussed at the 14th wave gauge from the wave paddles (Table 1), which was located at the front face of the model in its initial stationary location. As investigated by Baldock et al. (1996), non-linear wave effects mean that the location where wave groups actually focus differs from the input theoretical focus location ($x_{focus\_th}$). A trial and error process (as used by Ning et al., 2009) was used to adjust the theoretical focus location to bring the wave into focus at the required location ($\pm 0.05$ m). The wave is judged to be in focus at the position where the wave time history is symmetric i.e. the troughs on either side of the main crest have the same magnitude (Fig. 3). The theoretical focus locations necessary to achieve the required focus position in the wave basin are given in Table 2.

An alternative approach to achieve the required focus was initially proposed by Chaplin (1996). This requires measuring the phase of the wave group at the focus time at the required focus location, then iteratively adjusting the phase of each wave component to bring it closer to zero. For the wave groups used here this approach was not found to improve the focus of the wave group once the theoretical focus location had been adjusted. For example between 0.30 and 1.20 Hz (which incorporated 98% of the power of the wave group), for the ST4 case, the average normalised difference between the measured phase of the individual frequency components and the expected zero phase was 0.28° when adjusting the focus location only, and 0.37° when adjusting focussing location then phase.

The steepness of the wave group was increased further to generate the plunging breaking wave used for the second series of tests. The peak frequency of the underling PM spectrum was multiplied by 1.59, giving a theoretical steepness of $kA=0.35$, although the wave breaks before reaching this steepness. The point at which the wave breaks was varied by changing the theoretical focus location of the wave.

Testing breaking wave impacts at 50th scale introduces potential scaling effects. A number of studies have been conducted into these. Bullock et al. (2007) note that compressibility of air does not correctly scale and is less significant at smaller scales. Blenkinsopp and Chaplin (2011) report large differences in the 'temporal evolution of bubble plumes generated at model and full scale'. They found that the generated bubble plume dispersed quicker at smaller scale, potentially reducing the presence of entrained air within the water column. Bullock et al. (2007) state that the presence of air in the water column cushions the impact of waves breaking on walls, and therefore it can be expected that the differences in air compressibility and entrapment at 50th scale will introduce scale effects. It should be noted however that air entrapment from breaking waves is a cumulative effect. In this study a single plunging breaking wave is generated, therefore limiting the potential scale effects. Also, for the majority of cases in this study, the wave is breaking before impacting the model and therefore the effect of entrained air is expected to be limited at both model and full scale. Where the wave does break onto the model the impact pressures are reduced compared to impacts on a wall as the model can move in response to the wave. Again this will potentially reduce the influence of entrapped air and the associated scaling effects. Any scale effects that do occur as a result of testing at 50th scale are not believed to influence the validity at full scale of the conclusions made in regards to the use of single design waves to examine the response of a taut moored body to extreme waves.

## 3. Repeatability

Measurements using the breaking wave case, $kA=0.35$ wave group, with a theoretical focus location of 21.50 m, were repeated three times to assess repeatibility. Fig. 5 presents the results of these measurements.

The mooring force has been normalised by the force required to achieve maximum extension of the spring, 9.4 N. This was obtained using Hooke's law and the maximum possible extension of the mooring spring from its initial extension in calm water (147 mm). Three snatch loads were measured in each repeat run, represented by spikes in the recorded load. In this context snatch loads are defined as a spike in the mooring load caused when the mooring spring is extended to its maximum extension and the motion of the model restrained by the end stops.

The results demonstrate good repeatability during the intial interaction between the breaking wave and the model. However the difference between repeat results increases as time progresses in the experiment. The maximum difference between repeats in the magnitude of the first snatch load is 3%, while by the 3rd snatch load this has increased to 22%. A similar pattern can be observed in the device motions, with the difference in the magnitude of surge between repeats increasing from 2% for the first peak to 8% by the third peak. The maximum difference between repeats in pitch magnitude increases from 5% to 41% between the 1st and 4th peak.

This increase in the difference between the repeat measurements demonstrates that relatively small changes in the wave–body interaction can result in significant differences in body motion and load after only a few periods. The motivation for these tests is to investigate the wave–body interaction leading to extreme loading, and as this usually occurs in the early stages of the interaction, the quality of data is deemed acceptable.

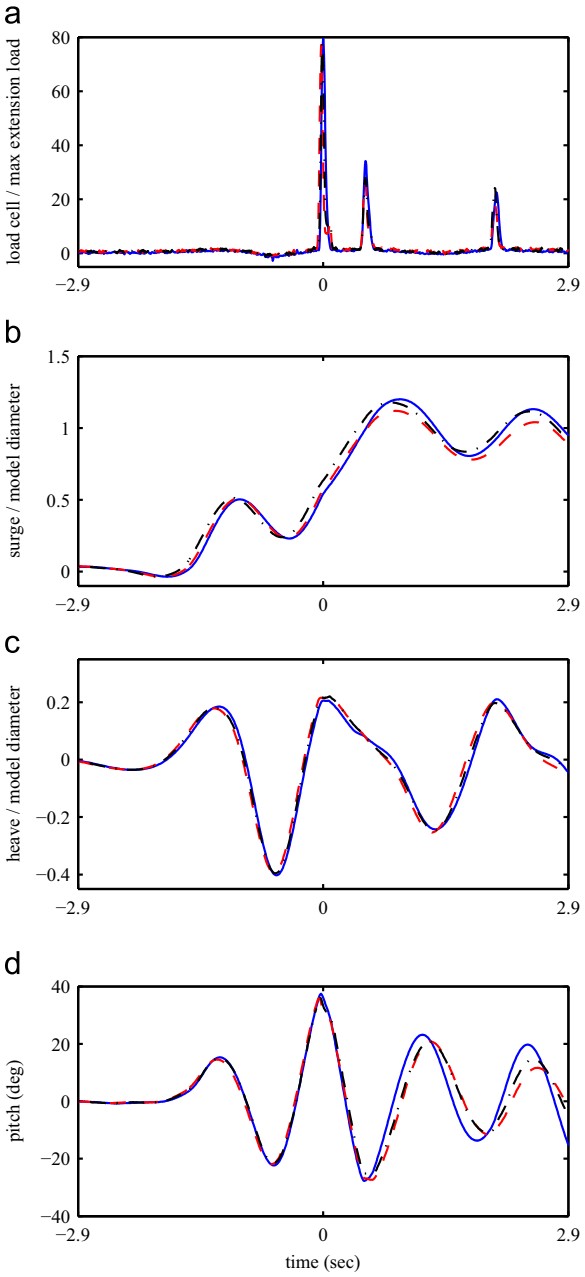


**Fig. 5.** Results from repeat measurements for $kA=0.35$ and $x_{focus\_th}=21.50$ m: (a) measured mooring loads, (b) surge, (c) heave and (d) pitch. Results from three repeats are presented.

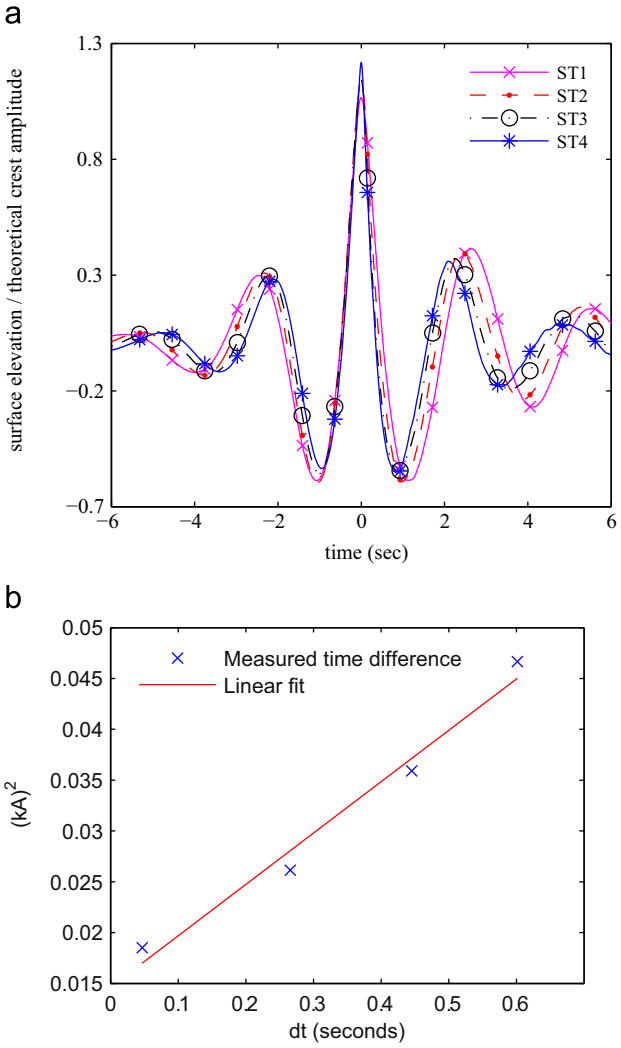


**Fig. 6.** Measured wave groups of increasing steepness.

**Table 3**
Properties of the non-breaking wave groups tested.

| *Case* | *kA* (theory) | *kA* (measured) | *A* (measured) (m) |
|---|---|---|---|
| ST1 | 0.150 | 0.167 | 0.285 |
| ST2 | 0.175 | 0.189 | 0.302 |
| ST3 | 0.200 | 0.203 | 0.303 |
| ST4 | 0.225 | 0.264 | 0.335 |

## 4. Experimental results – non-breaking waves

### 4.1. Wave measurements

Surface elevation time histories of the four non-breaking wave groups are shown in Fig. 6, measured at the resting location in still water of the front face of the model. The time series of each run has been shifted so that the main crest occurs at $t=0$ s at the focus location. As described above, the peak frequency of the underlying spectrum was multiplied by the frequency multiplication factors in order to increase the group steepness. A small increase in the amplitude of the main crest, from the theoretical value of 0.267 m, was also measured as the steepness increased, as seen in Table 3. Wave steepness was therefore also larger than predicted. These differences increase as the theoretical wave steepness increases, with measured steepness being 17.3% larger than predicted for ST4. At the focus location there is also a decrease in the wave troughs either side of the main crest, compared to that predicted by linear theory, for the two steepest cases (ST3 and ST4).

These findings are in agreement with those of Ning et al. (2009), who investigated the effect of wave steepness on NewWave type focussed wave formation. They also found that as wave steepness increased the main crest and surrounding troughs increasingly deviated from those predicted by linear theory (upon which the generation of the focussed wave groups in this study is based). Ning et al. (2009) state that this is due to non-linear wave–wave interactions (particularly 3rd order). No conclusive evidence was observed of the magnitude of higher order harmonics increasing as wave steepness increased in the spectrum of the measured signals (Fig. 7). However Ning et al. (2009) predict that 3rd order nonlinear interactions are the cause of the observed shift between the theoretical focus time and the

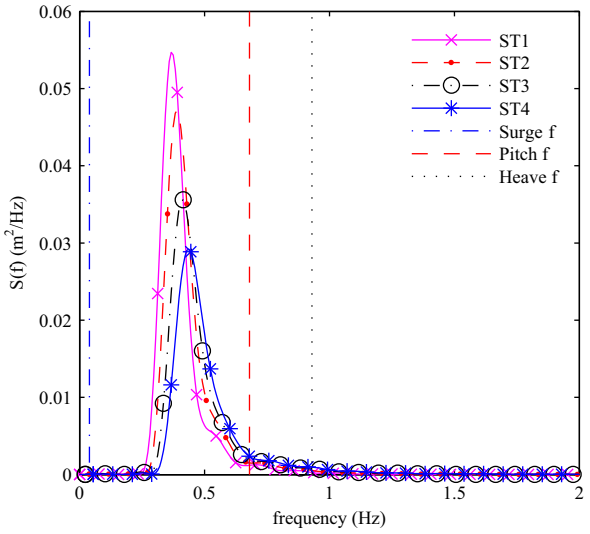


**Fig. 7.** Wave spectrum for the 4 wave records in Fig. 6. The resonance frequencies of 3 of the models degrees of freedom are also identified.

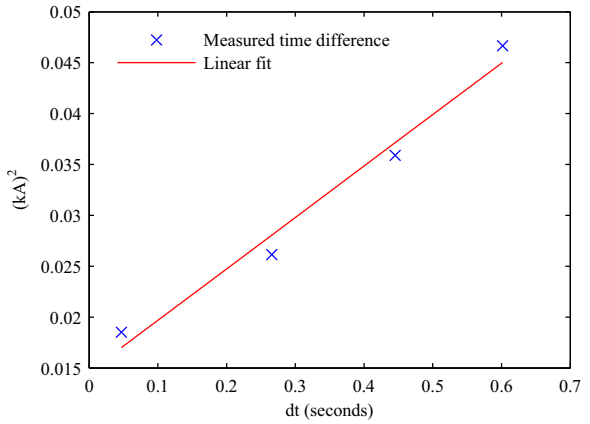


**Fig. 8.** Approximate linear relationship between wave steepness squared and the difference between theoretical and measured focussed time (d$t$).

actual focus time of generated wave groups, and that as such an approximate linear relationship should exist between this time shift and the square of the wave slope at focus. Fig. 8 demonstrates that this was indeed the case for the 4 wave groups tested here, indicating an increasing effect of non-linear wave–wave interactions as steepness increased.

### 4.2. Mooring loads

The measured mooring loads generated by the four non-breaking wave groups are presented in Fig. 9. Each wave group generated two snatch loads. The recorded time series has each been shifted in time and aligned so that the first snatch load occurred at $t=0$ s.

The magnitude of the first snatch load did not demonstrate a large dependence on wave steepness, with only a 4.7% increase between ST1 and ST4. The second snatch load demonstrated a greater dependence, with a 45.5% decrease between the least steep and steepest wave group. The relationship between wave steepness and the magnitude of the second snatch load was not however constant, with the difference being only 0.54% between ST1 and ST2 and much greater, 37.8%, between ST3 and ST4. There is also a time difference, with a delay of 0.45 s between the first and second snatch loads for ST1, increasing to 0.50 s for ST4.

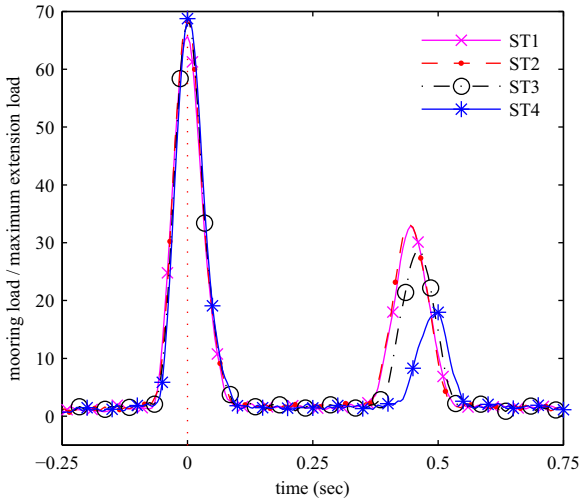


**Fig. 9.** Measured mooring loads generated by wave groups of increasing steepness.

The measured mooring loads are plotted alongside the wave groups measured at the focus location in Fig. 10. In this instance all the time series have been shifted by the same time so that the first snatch load during ST1 occurs at $t=0$ s. The shift in wave focus time as wave steepness increases (as presented in Fig. 8) can therefore be observed. It should be noted that as the model is displaced away from its initial equilibrium position the wave measured at the focus location is no longer identical to the wave impacting the model. Regardless, it can be observed from Fig. 10 that the first snatch load appears to be a direct result of the main wave crest, while the second snatch load occurs as the back edge of the main wave crest passes the body.

Fig. 11 examines this difference between the first and second snatch load in more detail. It plots the position of the floating body relative to the instantaneous free surface contour during both snatch loads for cases ST1 and ST4.

The instantaneous free surface contour corresponding to the time at which each load occurs is interpolated between the wave gauge measurements taken without the model present. It should be noted that reflections from the model will alter the surface elevation after the initial wave–model interaction and therefore this surface contour does not correspond exactly to the wave impacting the device. The first snatch load occurs as the leading edge of the main wave crest induces a heave in the model. Fig. 11(a) and (b) demonstrates that the model is in approximately the same location during the first snatch load for both values of wave steepness. The second snatch load occurred as the back edge of the main wave crest is passing the body. After the first snatch load the mooring retracts slightly and needs to be extended again before the second snatch load occurs. For case ST1 this occurs near the peak of the main wave crest. As the wave gets steeper, and the model is displaced further from its equilibrium position in surge, the second snatch load occurs further down the wave crest and with a greater horizontal displacement of the model. The wave imparts less force to the model, resulting in the observed smaller snatch load.

### 4.3. Device response

The response of the device recorded with the optical tracking system is plotted in Figs. 12–14. As with the mooring loads displayed in Fig. 9, the time series have been shifted so that the first snatch loads occurred at 0 s for all data series.

A much greater difference is found in the dynamic response of the model to the 4 different wave groups compared to the difference in mooring loads. The second peak in surge after the first snatch load is

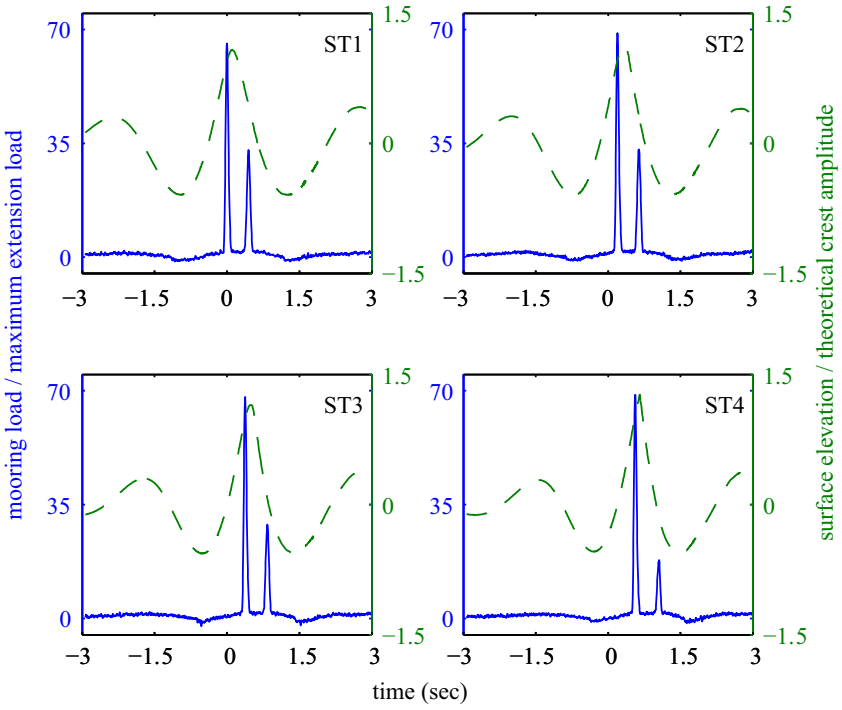


**Fig. 10.** Measured mooring loads plotted alongside the corresponding surface profile at the focus location.

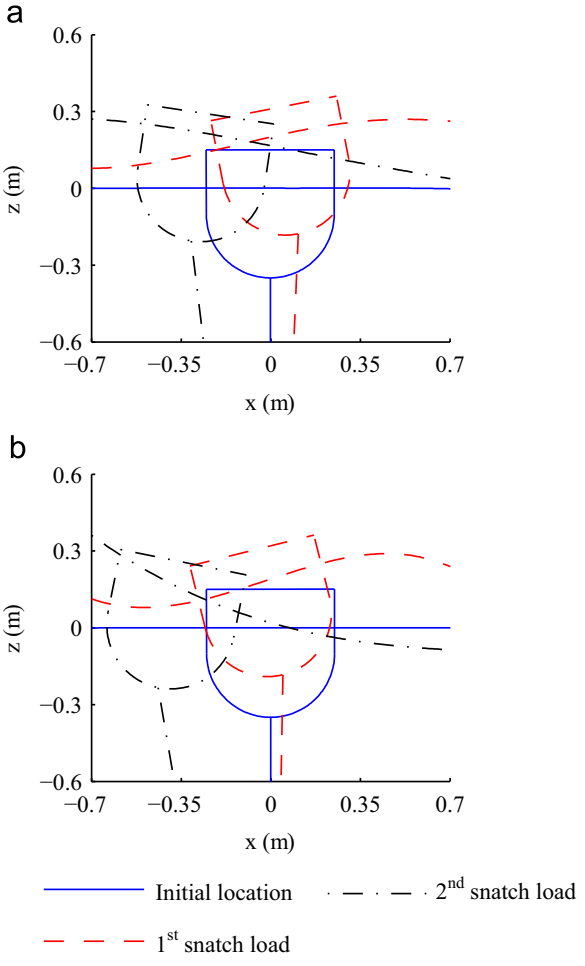


**Fig. 11.** Position of the model and the approximate instantaneous wave profile at the time of the first and second snatch loads, for cases (a) ST1 and (b) ST4.

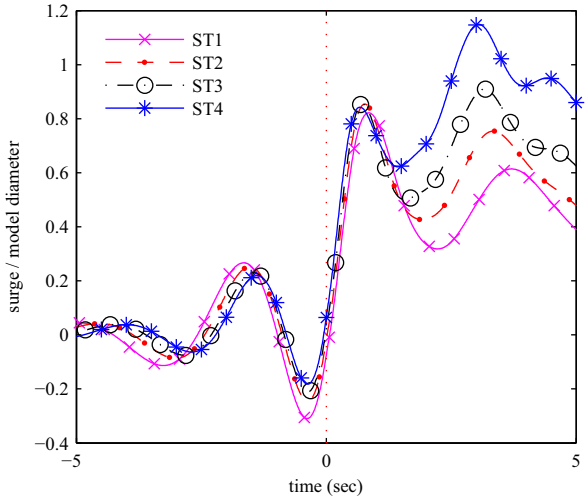


**Fig. 12.** Surge of model generated by non-breaking wave groups.

87.1% greater for ST4 than for ST1, while the first peak in pitch after the first snatch load was nearly three times larger for ST4 compare to ST1. This difference is likely due to a combination of wave steepness and the change in the spectral content of the wave group compared to the resonance frequencies of the model. In Fig. 7 the measured wave spectrum for each wave group is plotted, along with the 3 relevant resonance frequencies. The surge resonance frequency occurs at a significantly lower frequency then the peak frequency in each spectrum, with a low power which changes very little between each case. As such it can be concluded that surge response is increasing due to increasing wave steepness. The cause of the increase in pitch response between ST1 and ST4 is more complicated. In Fig. 7 it can be observed that as wave steepness increases the peak spectral frequency increases towards the pitch resonance frequency. It can therefore not be concluded whether the observed increase is due to this, the increased wave steepness, or a combination of the two.

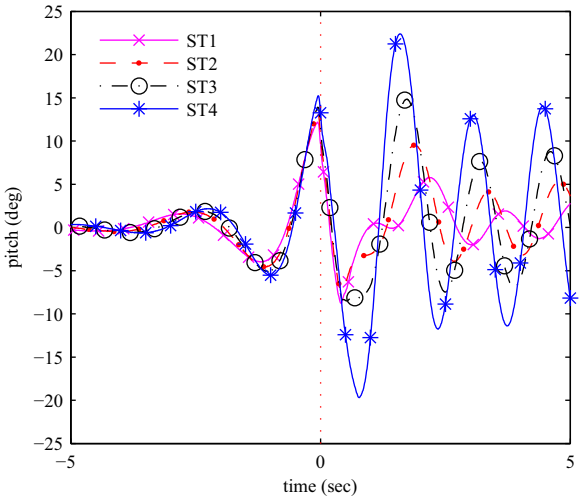


**Fig. 13.** Pitch of model generated by non-breaking wave groups.

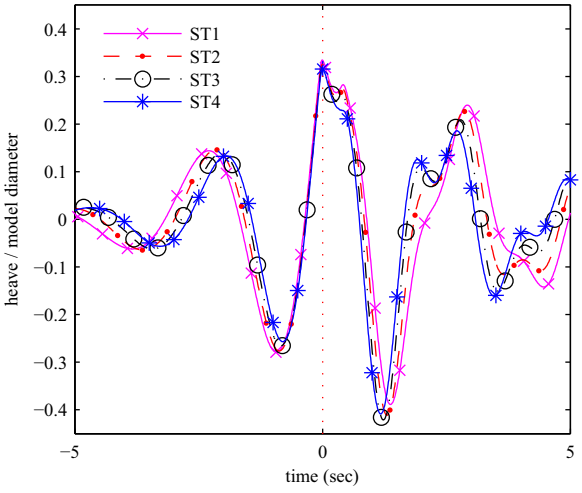


**Fig. 14.** Heave of model generated by non-breaking wave groups.

The change in heave response (Fig. 14) of the model between the 4 wave groups is less significant, with a 22.5% reduction between ST1 and ST4 in the peak heave which occurs approximately 2.8 s after the first snatch load. Between ST1 and ST4 the peak frequency of the wave groups moves closer to the heave resonance frequency. As such an increase in heave response might be expected. Instead the loading imposed by the mooring, shown in Fig. 9, has a much greater influence on heave than wave steepness and the change in excitation frequency.

A fast Fourier transform conducted on the measured motions for 60 s after the snatch loads occurred gave the resonance frequencies of the system. For all four cases these are in agreement with resonances measured in the free decay tests.

## 5. Experimental results – breaking waves

### 5.1. Wave measurements and breaking point

A series of 12 different theoretical focus locations ($x_{focus\_th}$) were used when investigating the effect of the plunging breaking wave on the model. Initial measurements of the wave groups using the probe arrangement given in Table 1 were used to estimate the wave breaking location.

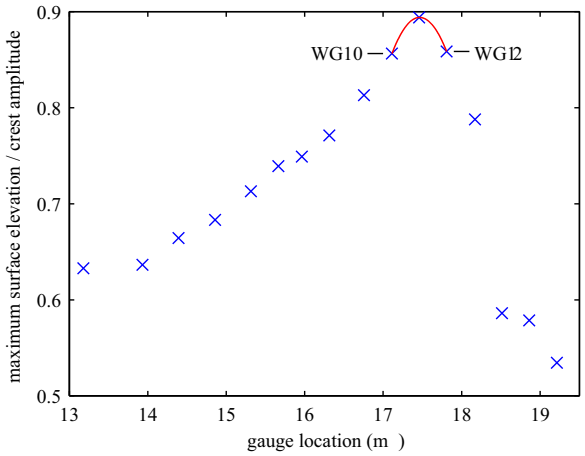


**Fig. 15.** Surface elevation of main crest measured at each gauge, when $x_{focus\_th}$=21.5 m.

**Table 4**
Breaking wave groups tested.

| Case | $x_{focus\_th}$ | $x_{break}$ | $x_{relative}$ |
|---|---|---|---|
| F1 | 23.00 | 19.00 | −0.24 |
| F2 | 22.75 | 18.75 | 0.01 |
| F3 | 22.50 | 18.50 | 0.27 |
| F4 | 22.25 | 18.24 | 0.52 |
| F5 | 22.00 | 17.99 | 0.77 |
| F6 | 21.75 | 17.74 | 1.02 |
| F7 | 21.50 | 17.49 | 1.28 |
| F8 | 21.00 | 16.68 | 1.78 |
| F9 | 20.50 | 16.48 | 2.29 |
| F10 | 20.00 | 15.97 | 2.79 |
| F11 | 19.50 | 15.47 | 3.30 |
| F12 | 19.00 | 14.96 | 3.80 |

Following Mukaro et al. (2013), the wave breaking location ($x_{break}$) is defined here as the point at which the amplitude of the breaking crest is the largest. In Fig. 15 the surface elevation of the main crest recorded by each wave gauge is plotted against the wave gauge location with respect to the wave paddles, for the case $x_{focus\_th}$=21.5 m.

The breaking point of the wave in this example occurred between the 10th and 12th gauge. After the 13th gauge the main crest had fully broken. A cubic interpolation was used between the gauge which measured the maximum surface elevation, and the gauge either side, to give an approximation of the breaking location (as shown in Fig. 15). From these approximations the relationship between focus location and breaking location was identified for each of the focus location cases and found to be given by:

$$x_{break} = 1.01x_{focus\_th} - 4.23,$$

with a coefficient of determination ($R^2$) value of 0.997. The relationship between focussing point and breaking point is linear, and approximately from 1 to 1.

Table 4 lists the various theoretical focus locations tested, and the corresponding breaking points. The distance of the breaking point relative to the centre of the resting location of the model is termed $x_{relative}$. A larger positive value of $x_{relative}$ corresponds to the wave breaking further from the model and closer to the wave paddles.

### 5.2. Mooring loads

The measured mooring loads are displayed in Fig. 16 for the 12 test cases listed in Table 4. The extension of the mooring has also

been plotted on the same time axis. This was calculated using the heave and surge of the mooring attachment point on the underside of the model, calculated from the optical tracking system measurements. The mooring extension has been normalised using the maximum possible mooring spring extension (0.147 m). The normalised wave elevation measured at the at-rest position of the front face of the model without the model in place is also plotted. These measurements were only taken for a subset of experiments and as a result are not available for all wave breaking locations tested. As with Fig. 11, it should also be noted that reflections from the model will alter the surface elevation after the initial wave–model interaction, and that once displaced from its initial position this free surface profile no longer corresponds exactly to the wave impacting the device.

Four distinct snatch loads can be identified for the four cases with wave breaking closest to the model (Fig. 16a–d), and are labelled I, II, III and IV. As the wave breaks further from the model only three (II, III and IV) and then eventually only two (II and IV), snatch loads are seen. The magnitudes of the four different snatch loads are plotted in Fig. 17 against $x_{relative}$. In Fig. 18, the wave crests are numbered for case F3 to aid the discussion. The main crest is the breaking wave and crests 2 and 3 are non-breaking waves following the main wave.

Different trends exist in the four different snatch loads. Snatch load I was generated by the plunging breaker itself, caused by the main crest of the focussed group. As the wave reaches the model in case F1 the main crest amplitude is still increasing as the breaking location of the wave group is approached. In case F2, F3 and F4 the crest amplitude is decreasing as it reaches the model, due to the wave starting to break before reaching the model, but is still sufficient to generate a snatch load. By case F5 the wave amplitude of the breaking wave has decreased sufficiently by the time it reaches the model for no snatch load to be generated.

Snatch load II was recorded for all the wave focus locations tested. Fig. 16 (cases F3, F5, and F7–F12) indicates that this snatch loading is generated by wave crest 2 (see Fig. 18). With the exception of case F1 and case F6, the general trend is for the magnitude of snatch load II to increase with $x_{relative}$ up to a peak in

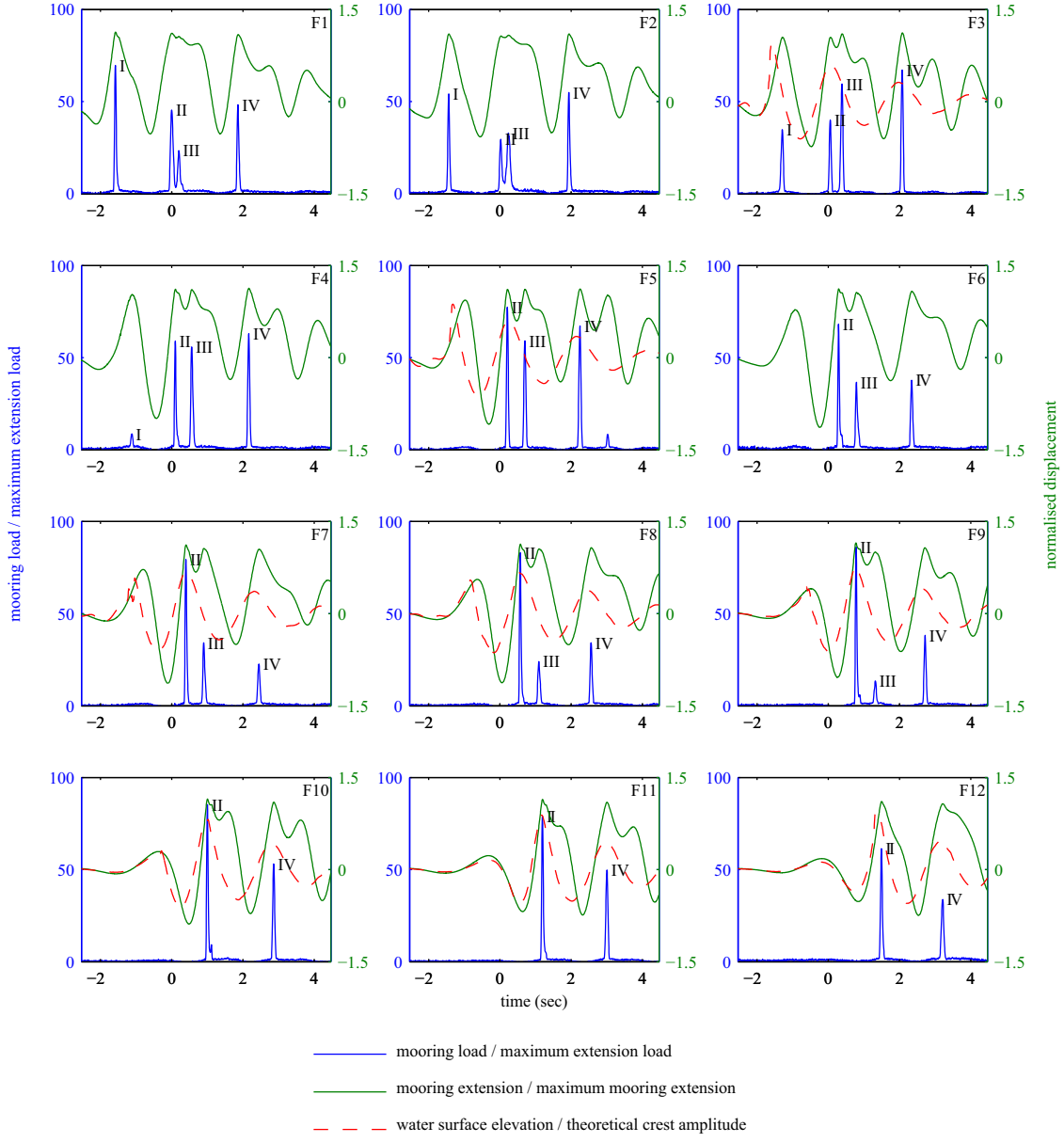


**Fig. 16.** Measured mooring loads, plotted alongside mooring extension and water surface elevation. Four different spikes in mooring load have been identified (I, II, III and IV). Note that the spacing between wave breaking points is not equal. Time series have been shifted so that snatch load II on case F1 occurs at 0 s.

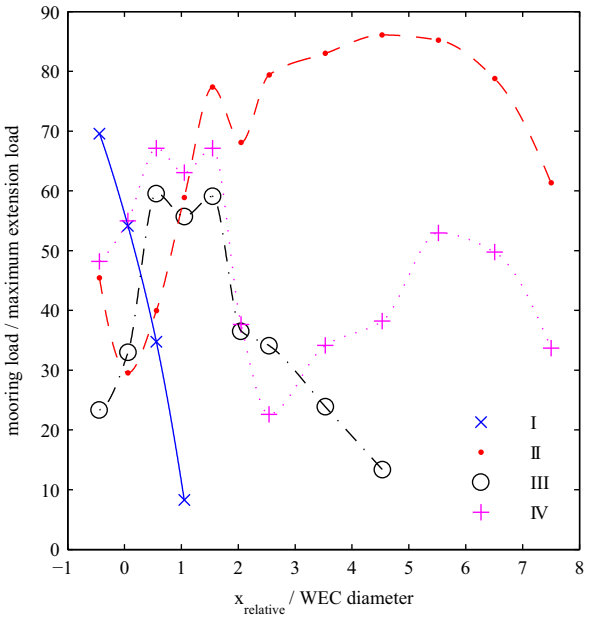


**Fig. 17.** Magnitude of the four mooring snatch loads, plotted against the wave breaking location relative to the model (normalised with the model WEC diameter). Mooring loads are normalised against the load required to achieve maximum mooring extension.

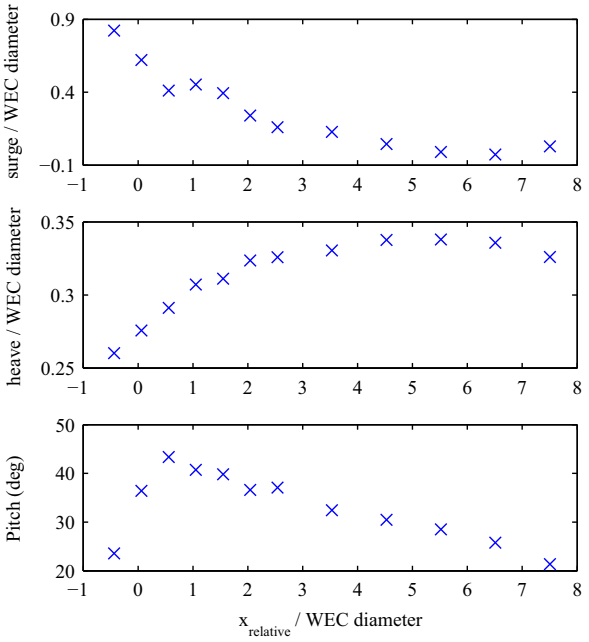


**Fig. 19.** Magnitude of 3 degrees of freedom at snatch load II. Heave and surge are for the mooring attachment point.

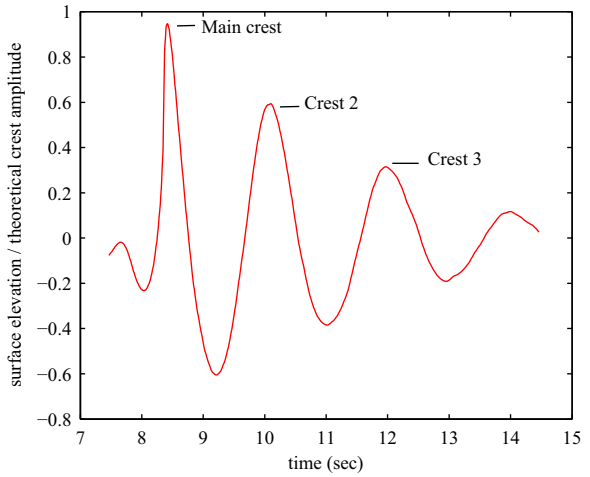


**Fig. 18.** Identification of main wave crest and wave crests 2 and 3 for case F3.

case F9. This increase is much greater between case F2 and case F5, when the wave breaks closer to the WEC, than between case F7 and F9.

In Fig. 19 the heave, surge and pitch motions of the model at the mooring attachment point are plotted against $x_{relative}$ at the time at which snatch load II occurred. Where $x_{relative}=0$, the wave breaks at the centre of the model in its resting position. Examples of how these motions relate to the wave profile are shown diagrammatically in Fig. 20. The closer to the model that the main crest breaks, the greater is its displacement from the initial position (indicated by a greater value of surge). This corresponds to a reduction in heave (as less heave is required to generate the maximum mooring extension and snatch load). Like surge, the pitch of the model at snatch load II reduces as the main crest breaks further from the model. The exception to this occurs for case F1 and F2, where the wave breaking onto the top of the model has damped the resulting pitch.

In Fig. 21 the pitch, surge and heave plotted in Fig. 19 are plotted against the magnitude of snatch load II. The steepness of wave crest 2 measured at wave gauge 14 (located at the front face of the model in its resting position) is also plotted against the magnitude of snatch load II. Wave steepness has been approximated by taking the difference between the zero-crossing time on either side of the crest as half the period then applying linear wave theory to obtain a value of $k$. The heave, and to a lesser extent surge, of the model can be seen to have the greatest correlation to the magnitude of the snatch load, while no obvious correlation exists for pitch. The wave steepness plot has two 'extreme values'. The first, with a snatch load of 39.9 N and steepness of 0.21, is the result from F3 where the main wave crest broke onto the model. The second, with a load of 61.3 N and steepness of 0.62, is the result from F12, where wave crest 2 starts to break in the vicinity of the model. If these values are removed a weak correlation between the steepness of wave crest 2 and mooring load is observed. This appears to be in agreement with the non-breaking results, where a small increase with wave steepness is observed in the first snatch load generated by a wave crest.

Snatch load II retards the model's motion and the mooring starts to contract. The third snatch loading, snatch load III, is then generated as wave crest 2 reverses this mooring contraction and the mooring is again extended to its maximum extension. The relationship between the second and third snatch load is complicated when the breaking point is close to the model. However as $x_{relative}$ increases from case F5 onwards and the steepness of wave crest 2 increases, the magnitude of snatch load III decreases. This is the same relationship as observed between wave steepness and the second snatch loading in the non-breaking data set above. Snatch load III does not occur after case F9.

The final snatch loading, snatch load IV, is generated by the next wave in the group (wave crest 3). By this stage the repeatability of the load measurements (Fig. 5) is significantly reduced. However an interesting observation can still be made. On its own the amplitude of wave crest 3 is not large enough to extend the mooring to its full extent, and hence generate a

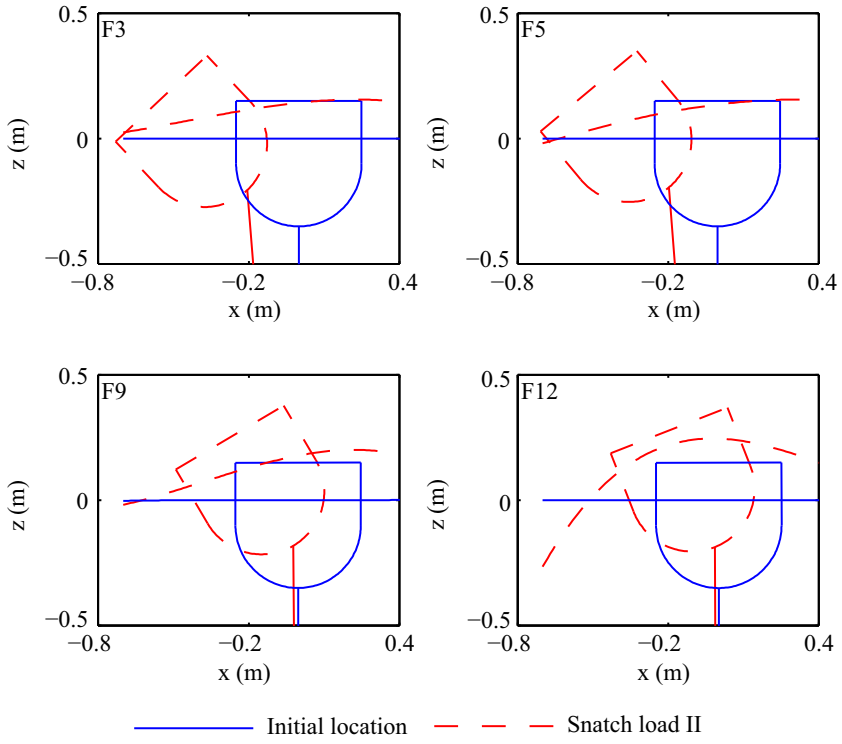


**Fig. 20.** Position of model when snatch load II occurs for cases F3, F5, F9 and F12.

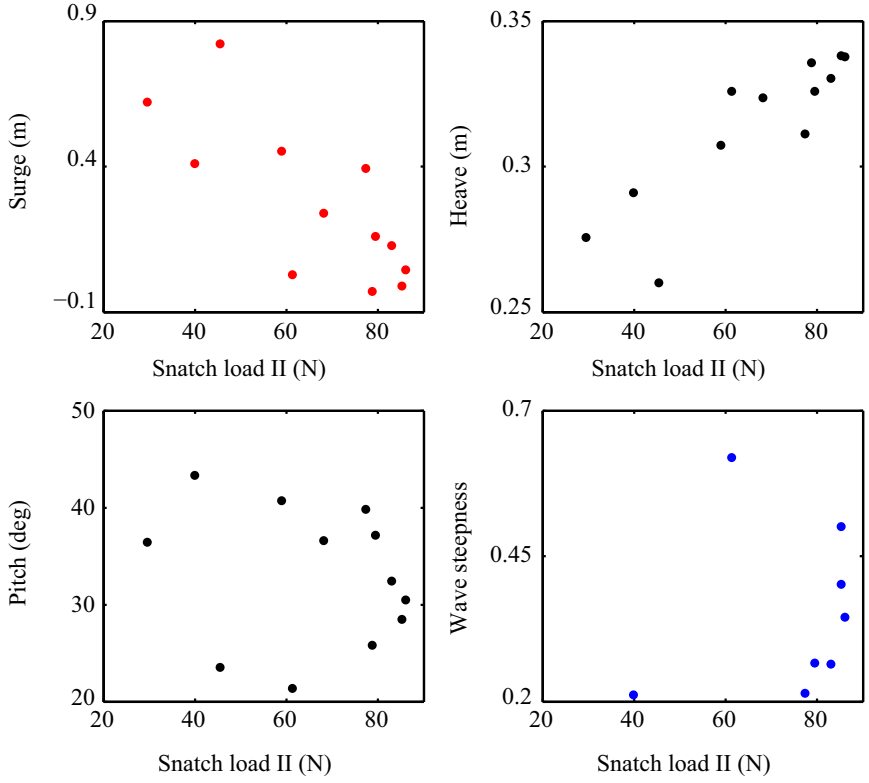


**Fig. 21.** Variation of surge, heave and pitch displacement and steepness of wave crest 2 with snatch load II.

snatch loading. Instead the displacement of the model from its initial position by the previous wave is required to partially pre-extend the mooring. This provides an example of how the mooring loads depend on the previous time history of the wave group.

Finally it should be noted that the largest mooring load occurred for case F9, when the wave broke 2.29 m from the model. This load was not however directly caused by the plunging breaker, but by a combination of the displacement caused by the breaking wave and the non-breaking wave following it.

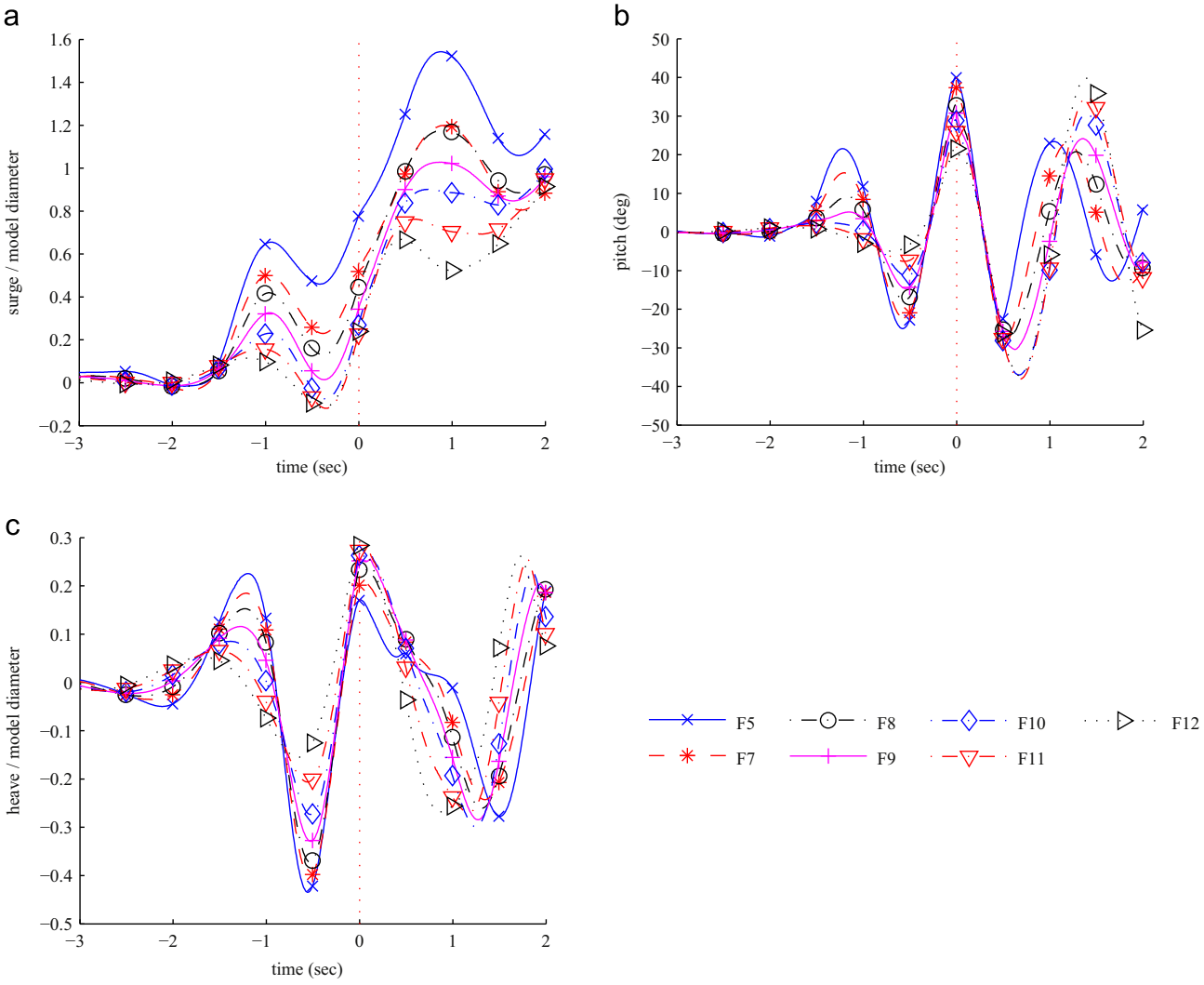


**Fig. 22.** Surge, pitch and heave of model generated by breaking waves.

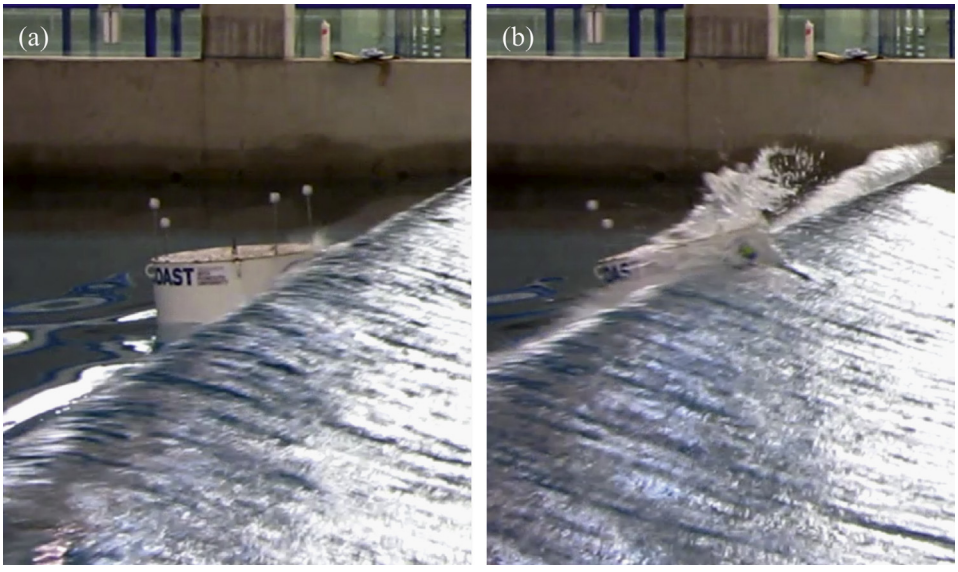


**Fig. 23.** Wave and model before (a) and after (b) wave slamming observed during case F5.

### 5.3. Device response

The time history of motion response for cases F5 and F7 to F12, in which the wave did not break directly onto the model, are shown in Fig. 22. Time series of surge, pitch and heave are given and are shifted in time so that the second snatch load is aligned at 0 s.

As expected, the further from the model the wave breaks, the more energy is dissipated before reaching the model, resulting in a smaller surge. The same effect can be observed in pitch before the occurrence of snatch load II. After snatch load II at $t=0$ the behaviour of the pitch is significantly different. At the first peak the order is reversed, with the wave that broke furthest from the model (case F12) generating the largest pitch, and case F8 the smallest. Snatch load II reverses the direction of the pitch motion (at 0 s). When the pitch is greater before snatch load II, a larger momentum has to be overcome to reverse this pitch, potentially explaining the smaller pitch magnitude observed afterwards.

For the three cases in Fig. 22(b) where the wave breaks closest to the model (case F5, F7 and F8) a phase difference in pitch between cases is also introduced after snatch load II. The cause of this phase difference is potentially generated by wave slamming caused by the breaking wave. Wave slamming on the side of the buoy was not directly measured, but was observed to occur when the wave broke close to the model (Fig. 23).

As was found for the surge response, the heave of the model before snatch load II follows a clear pattern, with a larger heave being generated the closer the wave breaks to the model. At snatch load II this pattern is reversed, the heave is lower and its direction reversed as the wave breaks closer to the model (with the exception of the small expansion of the Dyneema® mooring rope the maximum extension of the mooring at the snatch load is a fixed length). After snatch load II the difference in the magnitude and time at which snatch loads III and IV occur for the different experimental cases induces a phase difference between the oscillations in heave.

The resonance frequencies of the three degrees of freedom after the four snatch loads occur are the same as those recorded in decay tests.

## 6. Conclusions

Experimental measurements of focussed waves interacting with a single taut moored floating body representing a wave energy converter are presented. These focussed waves were designed to model extreme waves which exceed the design capacity of the mooring. The dependence of mooring load and device motion on both wave steepness and wave breaking point is explored.

The expected trends in motion with wave steepness are found. As the steepness of the central wave crest increases the resulting surge of the model also increases. Pitch also increases as wave steepness increases, although this is potentially influenced by a corresponding reduction in the difference between the wave excitation frequency and the pitch resonance frequency. It is significant that the initial NewWave (the least steep wave group tested) produced the smallest motion suggesting, for a body that responds as dynamically as the one tested here, that NewWave is insufficient to predict the extreme responses.

The effect of the breaking location of the plunging breaking wave on the surge of the model is also as expected, with less surge being generated the further the wave breaks from the model. The generated pitch and heave motions are found to be more complicated. Before any snatch loading occurred the larger motion amplitudes were generated by waves breaking closer to the model. However this pattern is reversed by the snatch load of the mooring, demonstrating the influence of snatch loading on the motion of a floating body.

Wave steepness is found to have only a minor effect on the magnitude of the initial snatch loading as the mooring spring's endstops were reached. The secondary snatch load generated by the falling edge of the main wave crest showed a greater dependency on wave steepness, with steeper waves generating less load. When investigating the effect of breaking wave location, a maximum of four snatch loads resulted from the incoming wave train. Only the first of these was caused directly by the plunging crest, and has a maximum measured amplitude within 1% of that of the non-breaking group. However the largest mooring load recorded occurs when the wave broke 2.29 m from the device and is generated by the smaller wave following the main crest. This leads to the conclusion that for a dynamically responding floating body (i.e. one that is able to move significantly away from its initial location) the mooring loads are dependent on the displacement history and as a result it may be concluded that a single focussed wave alone cannot be used to obtain an accurate assessment of extreme mooring loads.

The mooring used here was purposely designed to generate a snatch load. This allowed a worst-case scenario to be investigated and conclusions about the validity of using a single focussed wave to investigate extreme mooring loading to be drawn. Although snatch loading has been recorded during offshore measurements of wave energy converters (Savin et al., 2012) this was not generated directly by the mooring's capacity being exceeded, and a correctly designed device should not experience this form of loading. It is important therefore to design single taut moorings to avoid snatch loading and this requires knowledge of when snatch loading is likely to occur. These results demonstrate that the use of a single focussed wave as a design wave for extreme loading is insufficient to assess this.

This on-going study will next test a single taut mooring without the end stops present in this study. Snatch loading should therefore not be generated, although it is still expected that the single focussed wave approach will be insufficient to correctly investigate the extreme response. A series of measurements where the focussed wave is embedded into a random wave field, as first introduced by Taylor et al. (1997), are to be conducted and the resulting responses compared with the measurements presented here.

## Acknowledgements

This research was conducted as part of EPRSC project EP/J010235/1, X-MED: Extreme Loading of Marine Energy Devices due to Waves, Current, Flotsam and Mammal Impact. The principal investigator is Professor P.K. Stansby at the University of Manchester. The author would also like to thank the reviewers for their helpful feedback.

## References

Baldock, T.E., Swan, C., Taylor, P.H., 1996. A laboratory study of nonlinear surface waves on water. Philos. Trans. R. Soc. 354, 649–676.
Barstow, S., Mollison, D., Cruz, J., 2008. The wave energy resource. In: Cruz, J. (Ed.), Ocean Wave Energy – Current Status and Future Perspectives. Springer, Berlin.
Blenkinsopp, C.E., Chaplin, J.R., 2011. Void fraction measurements and scale effects in breaking waves in freshwater and seawater. Coast. Eng. 58, 417–428.
Borthwick, A.G.L, Hunt, A.C., Feng, T., Taylor, P.H., Stansby, P.K., 2006. Flow kinematics of focused wave groups on a plane beach in the U.K. coastal research facility. Coast. Eng. 53, 1033–1044.
Bullock, G.N., Obhrai, C., Peregrine, D.H., Bredmose, H., 2007. Violent breaking wave impacts. Part 1: results from large-scale regular wave tests on vertical and sloping walls. Coast. Eng. 54, 602–617.
Clément, A., McCullen, P., Falcão, A., Fiorwntino, A., Gardner, F., Hammarlund, K., Lemonis, G., Lewis, T., Nielsen, K., Petroncini, S., Pontes, M., Schild, P., Sjöström, B., Sørensen, H., Thorpe, T., 2002. Wave energy in Europe: current status and perspectives. Renew. Sustain. Energy Rev. 6, 405–431.
Chaplin, J.R., 1996. On frequency-focusing unidirectional waves. Int. J. Offshore Polar Eng. 6 (2), 131–137.
COAST Lab, 2013. Available: ⟨www.plymouth.ac.uk/coast⟩. (accessed 19.09.13.).

Elwood, D., Yim, S.C., Amon, E., von Jouanne, A., Brekken, T.K.A., 2011. Estimating the energy production capacity of a taut-moored dual-body wave energy conversion system using numerical modelling and physical testing. J. Offshore Mech. Arctic Eng. 133 (3), 031102 (9 pages).

Eriksson, M., Isberg, J., Leijon, M., 2006. Theory and experiment on an elastically moored cylindrical buoy. IEEE J. Ocean. Eng. 31 (4), 959–963.

Falcão, A.F.O., 2010. Wave energy utilization: a review of the technologies. Renew. Sustain. Energy Rev. 14, 899–918.

Halcrow, 2006. South West of England Regional Development Agency: Wave Hub development and design phase coastal processes study report. pp. 19.

Hunt-Raby, A.C., Borthwick, A.G.L., Stansby, P.K., Taylor, P.H., 2011. Experimental measurement of focused wave group and solitary wave overtopping. J. Hydraul. Res. 49 (4), 450–464.

Mukaro, R., Govender, K., McCreadie, H., 2013. Wave height and wave velocity measurements in the vicinity of the break point in laboratory plunging waves. J. Fluids Eng. 135 (6), 061303.

Ning, D.Z., Zang, J., Liu, S.X., Eatock Taylor, R., Teng, B., Taylor, P.H., 2009. Free-surface evolution and wave kinematics for nonlinear uni-directional focused wave groups. Ocean Eng. 36, 1226–1243.

Polinder, H., Scuotto, M., 2005. Wave energy converters and their impact on power systems. In: Proceedings of the International conference on future power systems. Amsterdam.

Ransley, E., Hann, M., Greaves, D., Raby, A., Simmonds, D., 2013. Numerical and physical modelling of extreme waves at Wave Hub. In: Conley, D.C., Masselink, G., Russell, P.E., O'Hare, T.J. (Eds.), Journal of Coastal Research. Special Issue No. 65, pp. 1645–1650, ISSN 0749-0208.

Rozario, J.B., Tromans, P.S., Efthymiou, M., 1993. Comparison of loads predicted using "NewWave" and other wave models with measurements on the tern structure. Wave Kinemat. Environ. Forces 29, 143–159.

Savin, A., Svensson, O., Leijon, M., 2012. Azimuth-inclination angles and snatch load on a tight mooring system. Ocean Eng. 40, 40–49.

Stallard, T., Taylor, P.H., Williamson, C.H.K., Borthwick, A.G.L., 2009a. Cylinder loading in transient motion representing flow under a wave group. Proc. R. Soc. A 465, 1467–1488.

Stallard, T.J., Weller, S.D., Stansby, P.K., 2009b. Limiting heave response of a wave energy device by draft adjustment with upper surface immersion. Appl. Ocean Res. 31, 282–289.

Taylor, P.H., Jonathan, P., Harland, L.A., 1997. Time domain simulation of jack-up dynamics with the extremes of a Gaussian process. J. Vib. Acoust. 119, 624–628.

Tromans, P.S., Anaturk, A., Hagemeijer, P., 1991. A new model for the kinematics of large ocean waves – application as a design wave. In: Proceedings of the 1st International Offshore and Polar Engineering Conference. Edinburgh, UK, pp. 64–71.

Walker, D.A.G., Eatock Taylor, R., 2005. Wave diffraction from linear arrays of cylinders. Ocean Eng. 32, 2053–2078.

Waters, R., Stålberg, M., Dabielsson, O., Svensson, O., Gustafsson, S., Strömstedt, E., Eriksson, M., Sundberg, J., Leijon, M., 2007. Experimental results from sea trials of an offshore wave energy converter. Appl. Phys. Lett. 90, 3.

Xu, L., Barltrop, N., Okan, B., 2008. Bow impact loading on FPSOs 1 – experimental investigation. Ocean Eng. 35, 1148–1157.

Zang, J., Taylor P.H., Tello M., 2010. Steep Wave and Breaking Wave Impact on Offshore Wind Turbine Foundations – Ringing Re-visited. IWWWFB25.

Zhao, X., Hu, C., 2012. Numerical and experimental study on a 2-D floating body under extreme wave conditions. Appl. Ocean Res. 35, 1–13.